Exploring the dynamics of remotely detected fluorescence transients from basil as a potential feedback for lighting control in greenhouses

A.-M. Carstensen[1], T. Wik[1], D. Bånkestad[2] and T. Pocock[3]

[1]Chalmers University of Technology, Göteborg, Sweden; [2]Heliospectra AB, Göteborg Sweden; [3]Smart Lighting Engineering Research Center, Rensselaer Polytechnic Institute, Troy, NY, USA.

Abstract

Optimizing artificial lighting control in industrial scale greenhouses has a potential for increased crop yields, energy savings and production timing. One possible component in controlling greenhouse lighting is continuous and accurate measurement of plant photosynthetic performance. A widely used tool for measuring photosynthetic performance non-invasively is chlorophyll fluorescence. For the purpose of automatic control, remote sensing of fluorescence is favourable, since it provides an aggregated measure for a large canopy area. However, adaptation of traditional fluorescence methodologies to remote sensing is problematic since they are based on the analysis of fluorescence intensities and therefore sensitive to distance and morphology. Other problems with using traditional methods remotely in a greenhouse are a need for dark adaption and use of saturating light. This paper presents a novel concept for the detection of photosynthetic performance based on the dynamics of remotely sensed light induced fluorescence signals. The dynamics of the fluorescence signal is insensitive to distance and morphology and hence provide a good basis for remote detection of photosynthetic performance. Through experiments we have explored how the dynamics of the time-varying fluorescence signal from basil plants was affected by light intensity, light acclimation and light induced stress. This was done by first identifying a dynamic model by transient analysis and then applying frequency analysis on the model. We conclude that the capacity of basil plants to use a certain light intensity was reflected by how fast and how complex the dynamics are. These results show that an identified resonance peak frequency is a potential indicator of plants' ability to adapt to light, which could be a valuable feedback signal for lighting control in greenhouses.

Keywords: chlorophyll fluorescence, photosynthesis dynamics, fluorescence transient, remote sensing, stress detection, light acclimation, supplementary light, greenhouse illumination, automatic control, black-box model, system identification

INTRODUCTION

Chlorophyll fluorescence (CF) is a widely used non-invasive probe of photosynthesis. The close relationship between CF and photosynthetic performance has made it an indispensable tool in studying photosynthesis in a wide range of applications, on-leaf as well as remotely from satellites. From lab-scale to the ecosystem-level CF is used to detect stress caused by various types of stressors such as drought, nutrient deficiency, pests and excess light (Murchie and Lawson, 2013; Porcar-Castell et al., 2014).

Conventional CF based methods analyse the CF response to a light pulse that fully saturates photosynthesis in dark-adapted plants. The methods are generally based on calculating index values from inflection points on the transient response curve (Strasser et al., 2000). Conventional CF parameters are advantageous in terms of their physiological interpretation. However, they do not use the full information available in the transient.

During the last decade it has been shown that different machine learning techniques applied to the 'continuous' CF transient are better at classifying plant stress and species

compared to conventional CF parameters (see Berger et al., 2006) for detection of plant pathogen infection; Blumenthal et al. (2014) for detection of drought, nutrient and chemical stress; Tyystjärvi et al. (2011) for differentiating between species). In these studies, the plant material has in general been dark-adapted before a fully saturating pulse was applied. An exception is Tyystjärvi et al. (2011), where the plant material was only "shaded" for 1 s prior to the saturating pulse, and Berger et al. (2006), where the excitation light was not saturating but was either 50 or 200 μmol m^{-2} s^{-1} photosynthetic photon flux density (PPFD).

Here we present a different and, in this context, novel approach where the 'continuous' CF transient response induced by an *excitation signal* is analysed in terms of properties of linear dynamic parametric black-box models fitted to the transient data (Ljung, 1999). By definition, an excitation signal causes a changing light intensity and is added to the ambient light intensity. This change can have different shapes, but in this work the excitation signal was shaped as a step-formed increase followed by a step-formed decrease in the incident light intensity. In this approach, the amplitude of the excitation signal can be kept relatively low (60 μmol m^{-2} s^{-1} PPFD). The CF transients are measured remotely by spectrometers generating an aggregate measure from the canopy area reached by the excitation light source. Furthermore, the measurements are performed on light adapted plant canopies and in the presence of ambient light.

The aim of the experimental work presented here was to explore how the dynamics of the CF signal is affected by ambient light intensity as well as by light induced stress. Responses from plants long term acclimated to (i.e., grown under) three different light intensities were studied and compared. This was motivated by our underlying goal to investigate the possibility to use changes in the CF dynamics as a feedback signal to control artificial lighting in commercial greenhouses.

In our previous work it was concluded that the CF response to a step-formed excitation signal was direction dependent, such that step increases and step decreases needed separate models (Carstensen et al., submitted). In the same study, an analysis of the CF response to step increases was presented, with three main conclusions: (i) increased ambient light intensity makes the transient response faster; (ii) plants long-term acclimated to a lower light intensity have a faster dynamics compared to plants acclimated to a higher light intensity; (iii) the overshoot of the transient response decreases upon light induced stress (as indicated by a decreased Fv/Fm).

Here we present the results for step decreases together with a comparison of step increases and decreases. Although the dynamics is not the same, an analysis of how the dynamics change with ambient light intensity and light induced stress shows the same pattern for step decreases as for step increases. Hence, the information from both increases and decreases can potentially be used for feedback to control artificial light in a greenhouse, meaning that it should be possible to at least halve the time needed to detect light stress with this approach. Based on this work, we also conclude that the resonance frequency and the amplitude of the resonance seem to be good signals to track in order to follow the plants' ability to cope with their light environment and stress.

MATERIALS AND METHODS

Plant material and growth conditions

Ocimum basilicum (sweet basil 'Nufar') was grown in three different growth units under L4AS1 LED-lamps (Heliospectra, Sweden) with incident light intensity set to 80, 250 and 500 μmol m^{-2} s^{-1} PPFD, respectively, and distributed into different wavebands as 2% UV 22% B, 10% G, 65% R and 0% FR. Light intensities and spectral distributions were measured with a calibrated JAZ spectrometer (Ocean Optics, Dunedin, FL, USA) without plants in the units. The photoperiod was 16 h.

Stress induction and recovery experiments

A stress induction and recovery experiment was performed on whole plants with 2-4 fully expanded pair of leaves under the L4AS1 LED-lamp. For the experiment, 24 pots with

5-7 plants in each were used. The experiment consisted of four consecutive phases with different ambient light intensity:

- Phase I: 110 µmol m^{-2} s^{-1} PPFD for 2.5 h;
- Phase II: 530 µmol m^{-2} s^{-1} PPFD for 1 h;
- Phase III: 1750 µmol m^{-2} s^{-1} PPFD for 2 h;
- Phase IV: 110 µmol m^{-2} s^{-1} PPFD for 3-6 h.

The ambient light in all four phases had the same spectral distribution as the LED growth light. Throughout the experiment an excitation signal (defined below) generated by the LED-lamp was added to the ambient light intensity. The experiment was repeated twice on each set of plants (from the three different growth units).

Continuously during the experiments incoming light, reflectance and fluorescence was measured remotely by spectrometers. Plant health was also regularly monitored through manual on-leaf measurements with a Pulse Amplitude Modulated chlorophyll fluorometer (PAM), for comparison with the remote sensing results.

The temperature was not controlled during the experiments and was between 22 and 24°C during Phase I and IV, 26°C during Phase II and 34-37°C during Phase III.

Excitation signal

Here we use the concept *excitation signal* for describing variations in the incident light intensity applied to induce variations in chlorophyll fluorescence. The excitation signal was generated by blue LEDs in the lamp (having peak maximum at 420 nm) and was shaped as a step-formed increase from 0 to 60 µmol m^{-2} s^{-1} PPFD followed by a step-formed decrease back to 0, repeated over and over again, forming a square wave with period time 600 s.

On-leaf PAM measurements

On-leaf CF measurements were made with a PAM (JUNIOR-PAM; Heinz Walz; Effeltrich, Germany) at room temperature on detached leaves. The youngest fully expanded leaves from 3 to 4 randomly distributed plants were picked and dark adapted for 20 min to fully oxidize QA. Minimum fluorescence (Fo) was measured using weak blue (450 nm) measuring light pulses while maximum fluorescence (Fm) was measured after a saturating blue (450 nm) light pulse of 10000 µmol m^{-2} s^{-1} PPFD for 800 ms. The ratio Fv/Fm was used to indicate changes in the maximum efficiency of PSII photochemistry due to photoinhibition, with Fv calculated as Fm-Fo (Krause and Weis, 1991).

Remote spectrometer measurements

Incoming light from the LED-lamp was measured at the canopy level by a Maya 2000 Pro Spectrometer (Ocean Optics, US) facing the lamp and equipped with a 50 µm optical fibre and a cosine corrector giving a field of view of 180°. Spectral radiance from the plant canopy (reflected light and fluorescence) was measured at a distance of 1 m from the plants by a QE65000 spectrometer (Ocean Optics, U.S.) equipped with a 600 µm optical fibre with a field of view of 25°. The sampling time was 0.2 s (on average). Further details are given in (Carstensen et al., submitted).

The intensity of the excitation signal at each time instant was calculated as the integrated absolute irradiance (µmol m^{-2} s^{-1}) in the wavelength interval 380-480 nm, measured by the spectrometer facing the lamp. For the radiance data collected with the spectrometer facing the plants, integrated absolute irradiance was calculated for the interval 700-780 nm, representing the fluorescence signal with a maximum at 740 nm.

System identification on step responses

The step responses were analysed in terms of properties of linear dynamic models. As was found for the step increase responses (Carstensen et al., submitted), the best-suited linear model structure was the Output Error (OE) model, which is described by

$$y(t) = \frac{B(q)}{A(q)}u(t) + e(t) \quad (1)$$

where $y(t)$ is the measured output (fluorescence), $u(t)$ is the input (the excitation signal), $e(t)$ is noise (for example measurement noise from the spectrometer), t is time instant (sample) and q is the forward shift operator. $B(q)/A(q)$ is a discrete time rational transfer function that defines the process model, i.e., the model of the response of the photochemistry to (any) changes in the incident blue light. B and A are polynomials in q. The order of the polynomial B defines the number of zeros of the process model, while the order of the A-polynomial defines the number of poles or, equivalently, the number of states in the process model.

The CF responses were different for step increases and step decreases, implying that the system is non-linear. This motivated an approach with separate model estimations to step increases and step decreases, while keeping each model linear. The linear modelling was implemented as an identification of the best suited model to each step, letting the model parameters, for a specified model structure and order, adapt as the dynamics of the photosynthesis changes due to altered physiology.

The search for a suitable model structure and model order followed the procedure described by Ljung (1999, Chapters 16 and 17). Estimation and evaluation of models were carried out using System Identification Toolbox in MATLAB (Ljung, 2007). The system identification procedure and the pre-treatment of data followed the procedure earlier used for step increases, as explained in detail in Carstensen et al. (submitted).

RESULTS AND DISCUSSION

Step decreases – time domain results

The CF responses to the step decreases were different at different ambient light intensities. Figure 1 shows selected responses to step decreases representative for the plants acclimated to 250 µmol m^{-2} s^{-1} and the different phases of the experiment. During Phase I and IV of the experiment, when the ambient light intensity is 110 µmol m^{-2} s^{-1}, the step decreases contain both a rapid dip and a slower oscillatory behaviour. In the step responses from Phase II of the experiment only the first rapid dip remains, although broadened, indicating that the dynamics is faster and less complex at the higher ambient light intensity (530 µmol m^{-2} s^{-1}) applied during Phase II. At the high ambient light intensity applied in Phase III (1750 µmol m^{-2} s^{-1}), the slow dynamics is completely lost and only the fast dynamics, seen through the initial dip, remains. These observations are valid also for the plants acclimated to 80 and 500 µmol m^{-2} s^{-1} PPFD (data not shown).

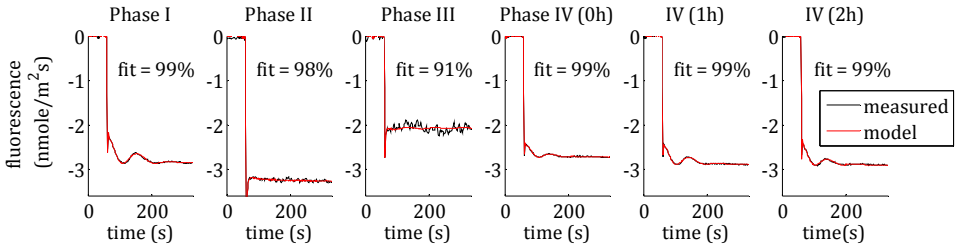

Figure 1. Fluorescence responses to step decreases from plants acclimated to 250 µmol m^{-2} s^{-1}. The curves are normalised and linearly detrended by the steady state levels preceding the step decreases. The figure shows one step from each of Phase I, Phase II, Phase III and three steps from Phase IV (first step during recovery, after 1 h of recovery, and after 2 h of recovery). Normalized mean squared errors in the simulated model output compared to the measured data are indicated as fit in percentage.

The amplitude of the oscillations appearing at low ambient light (110 µmol m^{-2} s^{-1}) turned out to be affected by light induced stress. At the end of Phase III and at the beginning of Phase IV the plants acclimated to 80, 250 and 500 µmol m^{-2} s^{-1} PPFD, were slightly photoinhibited and showed a decrease in the Fv/Fm of 19, 15 and 12%, respectively,

compared to the values measured at the end of Phase I. At the same time the amplitude of the oscillations in the remotely sensed CF was decreased compared to Phase I. During Phase IV the amplitude of the oscillations gradually increases (Figure 1) in parallel with that the plants are recovering almost to their pre-photoinhibitory Fv/Fm values (Table1).

There is one major difference between the plants acclimated to different light intensities. For the plants acclimated to 80 and 250 µmol m^{-2} s^{-1}, the response is faster than for the plants acclimated to 500 µmol m^{-2} s^{-1}. This is most clearly expressed at low ambient light where the frequency of the oscillations differed in such a way that the frequency was lowest for the plants acclimated to 500 µmol m^{-2} s^{-1} and highest for the plants acclimated to 80 µmol m^{-2} s^{-1}. This is shown in Figure 2 (left graph).

Table 1. Fv/Fm measured on-leaf at the end of the indicated phase of the experiment from plants acclimated to 80, 250 and 500 µmol m^{-2} s^{-1} as indicated.

Accl. to	Control	I	II	III	IV
80 µE	0.84	0.81	0.77	0.66	0.80
250 µE	0.85	0.83	0.77	0.70	0.83
500 µE	0.78	0.84	0.79	0.74	0.82

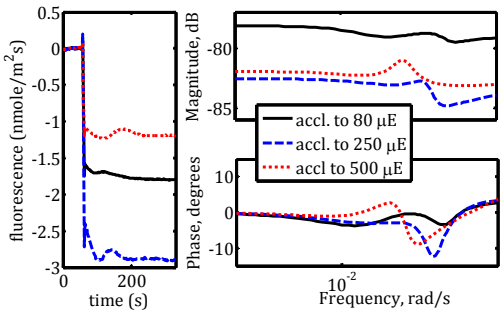

Figure 2. Step decreases measured under 110 µmol m^{-2} s^{-1} from plants acclimated to the different light intensities. Filtered raw data to the left and the corresponding estimated models seen in the frequency domain in bode plots to the right. Here µE is equal to µmol m^{-2} s^{-1}.

Step decreases – system identification

For step decreases under Phase I and IV of the experiment, 5 poles and 4 zeros gave the best fit in simulation. This could be compared with our previous work on step increases, where 3 poles and 3 zeros gave the best results (Carstensen et al., submitted). Hence, the complexity of the response to step decreases appears to be higher than the response to step increases. Under the highest light intensities (Phase III) the complexity of the dynamics decreased so much that the model order could be decreased to only 3 poles and 1 zero.

Step decreases – frequency domain results

A Bode diagram visualizes how much the model (Equation 1) predicts that the amplification is of a sinusoidal input (excitation light signal) of a given frequency, to the output (CF), and what the phase shift between them is (Figure 2, right graphs). The oscillations seen in the time domain appears as a resonance peak in the frequency domain. Hence, the effect of acclimation is seen as a movement of the resonance peak (Figure 2, right graph on top), such that the lower the light intensity of acclimation is, the higher is the resonance frequency.

The bode diagrams appeared to be affected by ambient light intensity in two ways. When the ambient light intensity was increased in Phase II (Figure 3) and Phase III (not shown), the bode diagrams were getting more flat indicating less complex dynamics. At the higher light intensities we also saw an increased amplification of higher frequencies

accompanied by a higher resonance frequency compared to low light intensities. This implies that the dynamics is faster at the higher light intensities. The resonance frequency as a function of PPFD is shown in Figure 4.

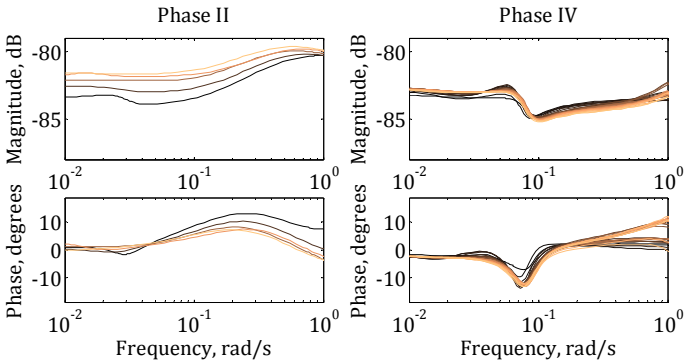

Figure 3. Models estimated to step decreases from the plants acclimated to 250 µmol m^{-2} s^{-1} seen in the frequency domain through bode plots. The color order goes from dark to light, indicating first to last step in the indicated experimental phases.

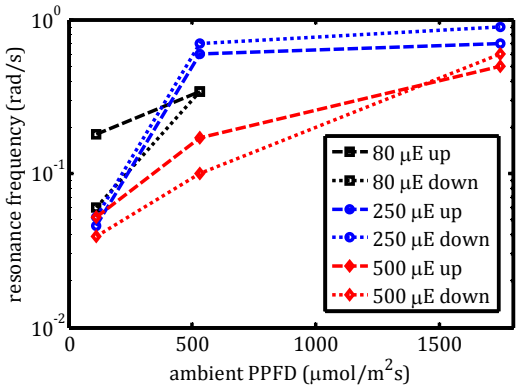

Figure 4. Resonance frequency at different light intensities for step increases and step decreases from plants acclimated to different light intensities, as indicated in the legend. The plants acclimated to 80 µmol m^{-2} s^{-1} do not have a resonance at the ambient PPFD 1750 µmol m^{-2} s^{-1}.

The amplitude of the resonance peak is successively changed both during Phase II and Phase IV of the experiment (Figure 3). During Phase II the resonant behaviour decreases for the plants acclimated to 250 µmol m^{-2} s^{-1}. This is seen through that both the magnitude and the phase plot of the bode diagram are gradually getting more and more flat for each step. This occurs in parallel with a 7% decrease in Fv/Fm (see Table 1). During Phase IV, the opposite behaviour is seen, with an increasing resonance peak in the magnitude plot and a decreasing minimum of the phase curve (Figure 3). This occurs at the same time as the Fv/Fm gradually increases again. The parallel increases in Fv/Fm and the amplitude of the resonance peak during Phase IV of the experiment is shown in Figure 5 and is most clearly expressed for the plants grown under 500 µmol m^{-2} s^{-1}. This trend is also clear during the first hour of recovery for the plants acclimated to 250 µmol m^{-2} s^{-1}. However, after the first hour of recovery, the resonance peak is again decreased. For the plants acclimated to 80 µmol m^{-2} s^{-1} the resonance is very small and the increasing trend during recovery is weak.

During Phase III the dominating dynamics is moved towards higher frequencies. At higher frequencies the noise level is higher, which is probably the reason why more variation between the models of individual steps is seen here, both in terms of resonance frequency

and amplitude of the resonance (data not shown). The fit in simulation is also significantly lower for models estimated to step decreases from Phase III (91% fit compared to 99% for the other experimental phases as indicated in Figure 1).

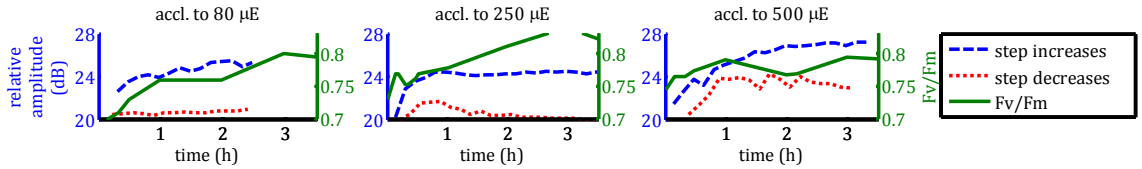

Figure 5. The relative amplitude of the resonance (left axis) during Phase IV of the experiment together with Fv/Fm values (right axis) measured on-leaf, for plants acclimated to different light intensities as indicated. The relative amplitude of the resonance is calculated as the maximum of the magnitude minus the magnitude at one fourth of the resonance frequency. The time axis indicates hours from the beginning of Phase IV.

Comparison of step decreases and step increases

The response to step increases and step decreases differs so much that the estimation of individual models for increases and decreases were motivated. Figure 6 shows the representative responses to step decreases and increases for Phase I and IV. Both the responses to step increases and step decreases contains a fast spike followed by slower dynamics. The response to step increases contains an overshoot and thereafter oscillations, whereas the response to step decreases contains no overshoot and only the oscillations (Figure 6, left graph). In the bode plot (Figure 6, right graph) this difference corresponds to a pure resonance peak for step increases while for the step decreases the resonance peak is followed by a decrease in the amplitude curve of the bode plot, attenuating the frequencies following the resonance. Furthermore, the modelling of the step decreases from Phase I and IV required one pole and one zero more than the modelling of step increases from these experimental phases.

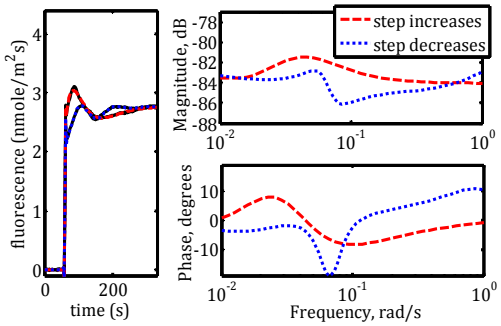

Figure 6. Fluorescence response to step increases and decreases representative for Phase I and IV of the experiment from plants acclimated to 250 µmol m^{-2} s^{-1}. Filtered raw data and simulated response in the time domain (left graph) and estimated models seen in the frequency domain (right graphs). The step decrease is plotted 'upside-down' in the time domain graph.

The step decreases from Phase II and III, on the other hand, contained the same dynamics as the step increases (data not shown), however, slightly shifted in the frequency domain. For the plants acclimated to 80 and 500 µmol m^{-2} s^{-1}, the response to decreases were generally slower than the response to increases. This agrees with the higher resonance frequency observed for step increases compared to step decreases (Figure 4). This was however not a general trend, since the resonance frequency is slightly higher for decreases than for increases for the plants acclimated to 250 µmol m^{-2} s^{-1}.

Apparently, the differences between step increases and step decreases are most pronounced during Phase I and IV, at low ambient light intensity, and less pronounced at the higher ambient light intensities applied during Phase II and III (data not shown). This is most likely a result of that the alterations in light intensity imposed by the excitation signal affects the ambient light intensity more (in percentage) at lower light levels. Another reason is that the dynamics that differs between step increases and step decreases is the slow dynamics, present only at the lower light intensities (Phase I and IV).

Although the responses to step increases and step decreases to some extent have different dynamics, they show the same trends. For both step increases and decreases, increased light intensity leads to faster and less complex dynamics. This is shown in Figure 4, where the resonance frequency is increasing with increased light intensity for all set of plants and for both step increases and decreases. Furthermore, for both step increases and step decreases the relative amplitude of the resonance peak seem to be related to light induced stress, measured as decreases in Fv/Fm (Figure 5). This behaviour is much more pronounced and is more consistent for the step increases than for the step decreases.

DISCUSSION

In our earlier work (Carstensen et al., submitted) we suggested that the observed behaviour, where the flow of energy (light intensity) in relation to the capacity of utilising energy (due to acclimation) determines how fast the system responds to an input signal, is typical for a system consisting of buffer volumes. We suggested that the buffers are metabolite pools. This observation is apparently valid also for the step decreases and probably, some states (buffers) are shared.

Here we have shown that the ambient light intensity affects the resonance frequency. We have also shown that the resonance frequency at a specific ambient light intensity is affected by the light intensity that the plants have been grown under and acclimated to. This makes us believe that the resonance frequency not only varies due to light level, but also due to light acclimation of photochemistry. What processes that actually govern the behaviour of the resonance frequency observed here need further examination.

The results presented here also show that long term light induced stress (decreases in Fv/Fm) can be detected through decreases in the resonance amplitude of the bode plot. Hence, long term physiological responses to light induced stress can be separated from the immediate effects of increased light intensity since the long term effects only affect the amplitude of the resonance and have almost no effect on the resonance frequency.

Furthermore, light intensity affects plants in combination with other growth factors, such as temperature, humidity and CO_2 concentration. Hence, a natural continuation of this work would be to explore how the dynamics of the fluorescence is affected by these parameters as well, together with a thorough analysis of photosynthesis through chlorophyll fluorescence analyses and actual CO_2 assimilation measurements.

Further work is needed to draw any conclusions about whether the non-linearities, that make the response to step decreases different from step increases, depend mainly on the relative changes in ambient light intensity imposed by the excitation signal. If so, it might be possible to adapt the amplitude of the excitation signal to the ambient light intensity such that the system response always is the same for step increases and step decreases. This would make the method investigated in this work faster and would open up for the use of standard recursive model identification.

CONCLUSION

The goal of this study was to explore how the dynamics of light induced fluorescence was affected by light acclimation, light intensity and light induced stress. Our results show that a method based on resonance frequency and resonance amplitude could provide important information about a plants capacity to cope with the current light intensity and their level of light induced stress, respectively. Such a method might provide appropriate feedback signals for automatic control of the light intensity in a greenhouse.

The dynamics of step increases and step decreases are slightly different, meaning that

separate identification of models to step increases and step decreases is necessary. However, the response to both step decreases and step increases contains the same information, meaning that light stress detection with the presented approach can be speeded up by using information from both decreases and increases.

ACKNOWLEDGEMENTS

The financial support for this work came from Mistra Innovation (www.mistrainnovation.se). The experimental work was carried out in the laboratory at Heliospectra AB (Gothenburg, Sweden), and we are very thankful to our co-workers there.

Literature cited

Berger, S., Benediktyová, Z., Matous, K., Bonfig, K., Mueller, M.J., Nedbal, L., and Roitsch, T. (2006). Visualization of dynamics of plant-pathogen interaction by novel combination of chlorophyll fluorescence imaging and statistical analysis: differential effects of virulent and avirulent strains of *P. syringae* and of oxylipins on *A. thaliana.* J. Exp. Bot. *58* (*4*), 797–806 http://dx.doi.org/10.1093/jxb/erl208. PubMed

Blumenthal, J., Megherbi, D.B., and Lussier, R. (2014). Unsupervised machine learning via Hidden Markov Models for accurate clustering of plant stress levels based on imaged chlorophyll fluorescence profiles & their rate of change in time. Paper presented at: IEEE Int. Con. on Computational Intelligence and Virtual Environments for Measurement Systems and Applications (CIVEMSA) (Ottowa, Canada; IEEE).

Carstensen, A.-M., Pocock, T., Bånkestad, D., and Wik, T. (in press). Remote detection of light tolerance in basil through frequency and transient analysis of light induced fluorescence. Computers and Electronics in Agriculture. (in press).

Krause, G.H., and Weis, E. (1991). Chlorophyll fluorescence and photosynthesis: the basics. Annu. Rev. Plant Physiol. Plant Mol. Biol. *42* (*1*), 313–349 http://dx.doi.org/10.1146/annurev.pp.42.060191.001525.

Ljung, L. (1999). System Identification - Theory for the User, 2nd edn (Upper Saddle River, NJ, USA: Prentice-Hall), pp.672.

Ljung, L. (2007). System Identification Toolbox for Use with {MATLAB} (Natick, MA, USA: MathWorks), pp.982.

Murchie, E.H., and Lawson, T. (2013). Chlorophyll fluorescence analysis: a guide to good practice and understanding some new applications. J. Exp. Bot. *64* (*13*), 3983–3998 http://dx.doi.org/10.1093/jxb/ert208. PubMed

Porcar-Castell, A., Tyystjärvi, E., Atherton, J., van der Tol, C., Flexas, J., Pfündel, E.E., Moreno, J., Frankenberg, C., and Berry, J.A. (2014). Linking chlorophyll a fluorescence to photosynthesis for remote sensing applications: mechanisms and challenges. J. Exp. Bot. *65* (*15*), 4065–4095 http://dx.doi.org/10.1093/jxb/eru191. PubMed

Strasser, R., Srivastava, A., and Tsimilli-Michael, M. (2000). The fluorescence transient as a tool to characterize and screen photosynthetic samples. In Probing Photosynthesis: Mechanism, Regulation and Adaptation, U.P.M. Yunus, and P. Mohanty, eds. (London, UK: Taylor and Francis), p.443–480.

Tyystjärvi, E., Nørremark, M., Mattila, H., Keränen, M., Hakala-Yatkin, M., Ottosen, C.-O., and Rosenqvist, E. (2011). Automatic identification of crop and weed species with chlorophyll fluorescence induction curves. Precis. Agric. *12* (*4*), 546–563 http://dx.doi.org/10.1007/s11119-010-9201-6.